ELSEVIER

Journal of Alloys and Compounds 453 (2008) 341–346

Journal of ALLOYS AND COMPOUNDS

www.elsevier.com/locate/jallcom

TEM studies of Nb_2O_5 catalyst in ball-milled MgH_2 for hydrogen storage

M. Porcu *, A.K. Petford-Long, J.M. Sykes

Department of Materials, University of Oxford, Parks Rd., Oxford OX1 3PH, UK

Received 20 July 2006; received in revised form 15 November 2006; accepted 16 November 2006
Available online 1 February 2007

Abstract

In this paper we report microstructural studies by transmission electron microscopy (TEM) of magnesium hydride nanocomposites produced by ball milling. The work employed high angle annular dark field (HAADF) imaging, high resolution TEM (HRTEM), and electron energy loss spectroscopy (EELS). MgH_2 samples had been prepared by ball-milling with 17 wt% of Nb_2O_5. Samples milled for a short time (30 h) show a decrease in particle size in comparison to MgH_2 milled alone for the same amount of time. After only 30 h milling, finely dispersed Nb_2O_5 was detected within the MgH_2 matrix. After milling for longer times (300 h) the amount of Nb_2O_5 dispersed within the Mg matrix increases. Analysis of material that had been milled for 300 h and then subjected to hydrogen desorption by heating showed that MgH_2 and Nb_2O_5 interact during the thermal desorption forming both a partially reduced niobium oxide phase and a mixed Nb-Mg-O phase.

Keywords: Hydrogen storage; Magnesium hydride; Niobium oxide; Transmission electron microscopy

1. Introduction

Magnesium hydride is a promising material for use in hydrogen storage because of the high hydrogen uptake (7.6 wt%). However, relatively high temperatures are needed during the hydrogen absorption/desorption cycle and reaction is slow, for example around 50 h are necessary to completely transform magnesium into magnesium hydride at 350 °C [1].

In the last few years, high-energy ball milling [2] and the addition of transition-metal (TM) and transition metal oxide (TMO) catalysts [3,4] have been used to improve the speed of reaction. Even when milled by itself, magnesium hydride shows improved kinetics relative to unmilled material, as a result of a particle/crystallite size effect: a decrease of particle size leads to a higher surface area, i.e. more nucleation sites for the hydride [2]. Moreover during mechanical alloying the material is heavily deformed introducing crystal defects such as dislocations, stacking faults, vacancies and an increased number of grain boundaries. These features enhance the diffusivity of hydrogen into the matrix [6]. It has been proposed that addition of TMs such as Ti and Nb make the hydrogenation/dehydrogenation process faster because these metals can form hydrides that act as a gateway for hydrogen breaking/recombination at the Mg/MgH_2 particle surface respectively [3–5]. Additions of TMOs also improve the hydriding/dehydriding kinetics by enhancing H-diffusion throughout the Mg matrix [4], and the hardness of the TMOs may help the particle size reduction process [7]. An additional factor is that the TMOs are cheaper than the corresponding TM and effective at lower levels of addition. The fastest kinetics have been reported by Barkhordarian et al. who showed that magnesium can absorb 7 wt.% of hydrogen in 1 min when pre-milled with 0.5 mol% of Nb_2O_5 [8]. So far however the exact mechanism that leads to such fast kinetics is unknown, and the microstructural changes involved during absorption/desorption cycles remain unclear.

X-ray diffraction methods have been the most widely used technique for studying the microstructural properties of both hydride and catalysts [5], but transmission electron microscopy (TEM) is able to characterise the size and distribution of individual phases [9], and has been used successfully to study metal hydrides [10–13]. Complex hydrides, such as $LiAlH_4$ seem to be stable under the electron beam [11] but Bokhonov et al. [10] and Herley and Jones [13] showed using electron diffraction that an electron beam easily triggers decomposition of MgH_2 in the TEM column.

In this paper we present results on the microstructure of a MgH_2-Nb_2O_5 nanocomposite formed by ball-milling. HAADF,

* Corresponding author. Tel.: +31 15 2786702; fax: +31 15 2786600.
E-mail address: m.porcu@tnw.tudelft.nl (M. Porcu).

0925-8388/$ – see front matter © 2006 Elsevier B.V. All rights reserved.
doi:10.1016/j.jallcom.2006.11.147

EELS, and HRTEM techniques have been used to analyze the microstructure with high spatial resolution.

2. Experimental details

Powders of ball-milled MgH_2 and Nb_2O_5 were supplied by GKSS Research Centre, Geesthacht, Germany). The powders were produced by milling together commercially available MgH_2 (97% pure, the remaining being MgO and Mg) and Nb_2O_5 (99% pure) powders (both from Alfa Aesar) for either 30 or 300 h in a Fritsch P7 Planetary Mill. The ball-to-powder ratio (BPR) was 10. A portion of the 300 h milled sample was subjected to thermal desorption by heating the powders to 300 °C in 30 min under H_2 pressure of 8 atm; then the vessel was evacuated to start the desorption. This characterizes the material that would be subjected to rehydriding in practical hydrogen storage and produces samples that are not subject to decomposition during TEM observation.

Sample preparation was carried out inside a nitrogen glove box because of the air-sensitive nature of the MgH_2 powder. The powders were ground under hexane to create a suspension. A drop of solvent plus powder was placed on an amorphous carbon film on a Cu TEM grid, then transferred into the TEM column when solvent was still present on the grid, in order to minimise as much as possible the exposure to air. This procedure reduces significantly the risk of oxidation. In any case small amounts of air during the milling process form a very thin layer of oxide that prevents further oxidation.

HRTEM, HAADF and EELS were carried out using a JEOL 3000F field-emission gun (FEG) TEM (point resolution 0.16 nm) equipped with a Schottky field emitter and operated at 300 kV. This microscope is fitted with a Fischione HAADF detector that collects the high-angle inelastically scattered electrons to form an incoherent image in which the contrast is a function of atomic number, z (so-called 'z-contrast' images). The machine is also equipped with a Gatan imaging filter (GIF) and a 2k × 2k pixels 794IF/20 MegaScan CCD camera. The GIF camera can be used for chemical analysis by acquiring a full EELS spectrum across the CCD array at each point in the analysis; the spectra were collected in scanning TEM (STEM) mode.

Energy dispersive X-ray (EDX) analyses have been carried out on a dedicated VG HB501 FEG STEM operated at 100 kV, equipped with an Oxford Instruments energy-dispersive X-ray spectrometer with a super atmospheric thin window.

3. Results and discussion

3.1. Effect of milling time

The structures reported here refer to the grain structure of Mg, rather than MgH_2 because, as previously reported [13], in the TEM hydrogen atoms are knocked-out by the electron beam leading to decomposition: several attempts were made using different voltages from 80 to 400 kV, but even at 80 kV the decomposition time prevented high resolution micrographs from being recorded. At 400 kV, in spite of a smaller scattering cross section than 80 kV, the decomposition proved even faster, clearly indicating a knock-on damage mechanism.

Table 1 reports structural data for Mg rather than MgH_2 as the latter decomposes quickly in the TEM column; however, since the ring width in the diffraction patterns was found to be the same for MgH_2 before and Mg immediately after decomposition, the Mg grain size can be used to infer the MgH_2 ones. It seems reasonable that the Mg preserves the grain structure of the original hydride. Preliminary examinations comparing MgH_2 milled alone for 30 h with MgH_2/Nb_2O_5 milled for the same time (labelled 30 h BM) showed only a slight decrease in MgH_2 particle size; such an effect has been attributed to the hardness of the oxide which assists cracking of the MgH_2 particles into smaller ones [7]. The particle size distribution of the hydride + catalyst sample ranges from 1 μm to 100 nm and the average value is 750 ± 95 nm after 30 h, compared to 1 μm for the sample milled for the same amount of time without catalyst. Note that each particle consists of an agglomerate of many nanoscale crystals (grains). Table 1 demonstrates also that the crystallite size of MgH_2 has almost reached its minimum value after 30 h; longer milling, i.e. 300 h, does not further reduce the crystallite size. The values for crystallite size were measured by taking dark field micrographs of Mg 1 0 0, 0 0 2 and 1 0 1 reflections; more than 400 crystallites have been used to calculate each average value.

The TEM bright field image seen in Fig. 1 shows the presence of dark particles embedded in the Mg matrix. These were identified as Nb_2O_5 by EDX analysis. Both Nb_2O_5 and MgH_2 are brittle and during the milling process fragments of the more brittle material (Nb_2O_5) become embedded in the less brittle MgH_2 [6]. A HAADF image of Nb_2O_5 particles is shown in Fig. 2a and b. The bright contrast regions can be identified as Nb_2O_5 particles, because the HAADF signal, generated by inelastic scattering depends on the atomic number (z), thickness (t) and density (ρ) of the sample. The phase containing the heavier element (Nb) gives the brighter contrast [14]. The detector geometry and its position inside the TEM column prevent Bragg-diffracted beams from being detected, thus forming a

Table 1
Particle size and crystallite size as a function of ball milling time (BM) in hours

	30 h BM	30 h BM Nb_2O_5	300 h BM Nb_2O_5
Mg particle size (nm)	1000 (103)	750 (95)	650 (78)
Mg crystallite size (nm)	30 (12)	13 (8)	12 (6)

Bracketed figures indicate standard deviation.

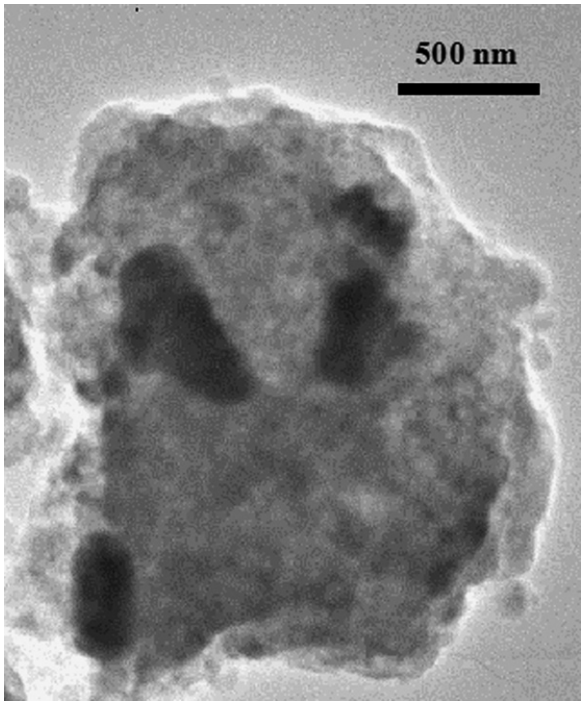

Fig. 1. MgH_2/Nb_2O_5 milled for 30 h. Bright field micrograph.

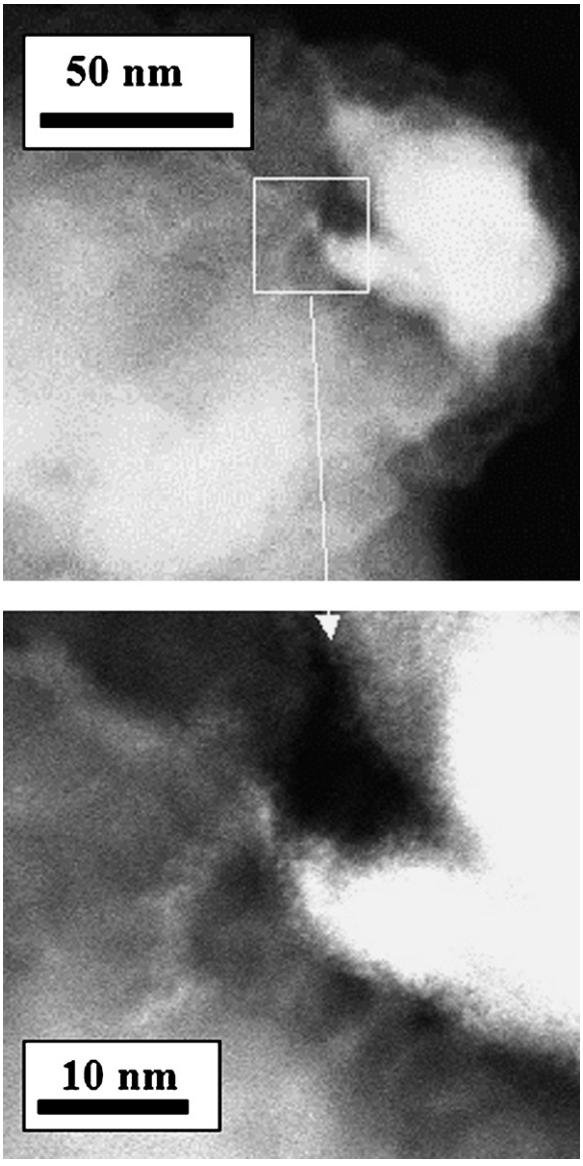

Fig. 2. MgH_2/Nb_2O_5 milled for 30 h. HAADF micrograph of an embedded Nb_2O_5 particle showing, in the enlarged image, the existence of a network of white features around the catalyst particle.

z-contrast image virtually free from diffraction contrast effects. In addition to the Nb_2O_5 particle, the enlarged image clearly shows many smaller white features in the vicinity of the particle. The shape of these features is such that thickness effects can be discounted. We therefore believe that the contrast observed in these features is due to Nb in some form at the Mg crystallite grain boundaries. This is supported by EDX point analyses (the probe diameter was 30 nm) that show Nb X-rays not only where the Nb_2O_5 particles could be seen, but also where no individual oxide particles could be distinguished in the TEM images. Calculations from the EDX data show that the Nb level within the Mg matrix is approximately 1 wt%. The minimum detectable level is about 0.3 wt%.

If the milling time is increased to 300 h, there is only a slight further decrease in Mg particle size as seen in Fig. 3 and in Table 1, with the average particle size now being around

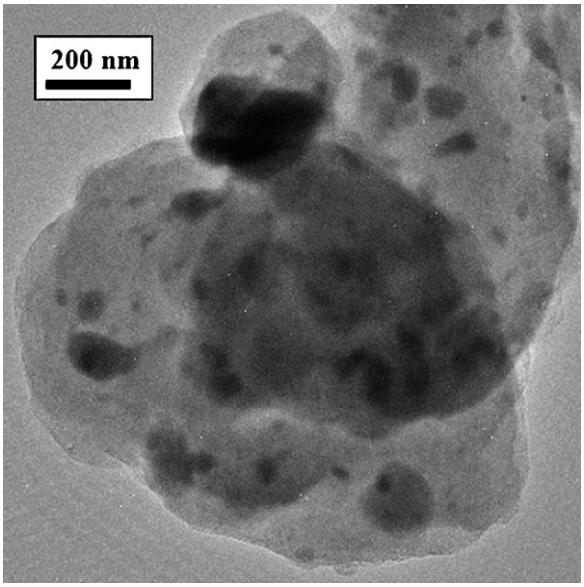

Fig. 3. MgH_2/Nb_2O_5 milled for 300 h. Bright field micrograph suggesting that most of the niobium oxide particles are embedded within the MgH_2 matrix.

650 ± 78 nm (as compared to 750 nm after 30 h milling). The size distribution is still broad, with particles ranging from 100 to 2000 nm visible in the TEM images. This is consistent with a continuous breaking and rewelding of the powder during the ball milling process [6]. These results seem to show that the milling process reduces particle size to an essentially constant diameter after not much more than 30 h.

The catalyst distribution after 300 h milling is more homogeneous than it was after only 30 h milling: the majority of the oxide particles are reduced in size and embedded within the hydride matrix. The HAADF image shown in Fig. 4 indicates the existence of three main types of Nb_2O_5 feature: large particles (bigger than 200 nm in diameter) such as 1, small particles less than 200 nm fully embedded on the Mg matrix surface

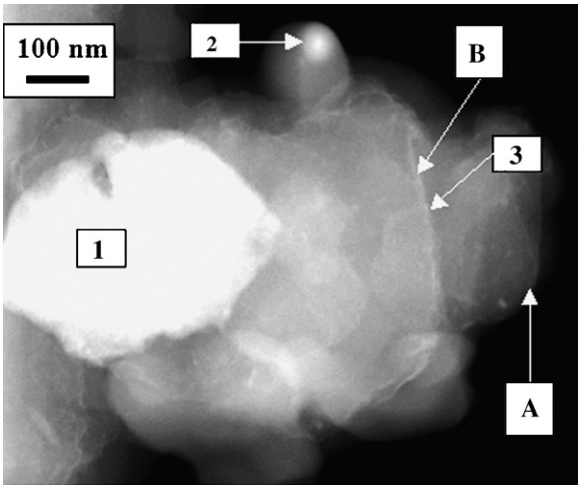

Fig. 4. MgH_2/Nb_2O_5 milled for 300 h. HAADF micrograph of MgH_2 particle demonstrating that Nb_2O_5 exists in two different size distributions, indicated by 1 and 2. Label 3 indicates bright Nb_2O_5 features. Labels A and B refer to the EELS spectra shown in Fig 6.

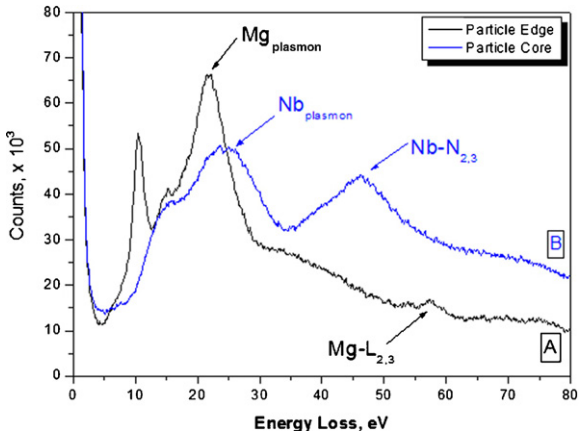

Fig. 5. MgH_2/Nb_2O_5 milled for 300 h. EELS spectrum of (A) magnesium hydride particle edge and (B) white features. The labels refer to Fig. 4.

(labelled 2) and bright Nb-rich features (labelled 3) which appear to be finely distributed within the hydride phase, but in particular delineate the edges of Mg crystallites in the matrix. As previously indicated, the position of the lines and the abruptness of the contrast is such that we do not believe it possible for them to arise from a thickness effect. EDX elemental maps for the sample milled for 300 h show that the amount of the Nb-based phases within the Mg matrix is now ~2 wt%. The experimental error (around 0.3 wt%) allows to say that there is an increase of Nb-based compounds within the Mg matrix (from 1 to 2 wt%) due to the milling process and that the bright regions are likely to be Nb-rich. These bright regions in the HAADF images identify areas of particular interest for study in greater detail by HRTEM or EELS, which was subsequently able to confirm the identity of some of these features. The ability to select such areas for further study was a particular benefit of HAADF imaging.

The EELS experiments were focused on analysis of the low-loss region of the spectrum (0–80 eV energy loss). The spectra labelled A and B in Fig. 5 were collected at the points labelled A and B in Fig. 4. Low-loss spectra from pure Mg, Nb_2O_5 and Nb, though not shown here, were also collected for comparison with spectra from our samples. At the Mg particle edge (spectrum A), the Mg plasmon peak and the Mg $L_{2,3}$ edge are clearly detected. The peak at ~10 eV is attributed to oxygen, as the oxygen K-edge is also present at ~530 eV (not shown in the figure). The presence of oxygen comes from the powders themselves: X-ray diffraction analyses of the commercial MgH_2 powders detected a fine-grained MgO (3–4 wt%) [15]. In addition, a surface layer of MgO may well come from the handling procedures [12].

Spectrum B, recorded on one of the bright line features, confirmed that these do indeed consist of Nb_2O_5; the low-loss spectrum exhibits details that can be identified as corresponding to Nb_2O_5 with both the characteristic plasmon peak and the N_{2-3} edge clearly detected. Because of the strong ionic character of both MgH_2 and Nb_2O_5 it is possible for interaction to happen during the milling process, promoting diffusion through the Mg matrix [16]. The finely dispersed Nb_2O_5 and its highly defective structure suggest firstly that it may provide easy pathways for hydrogen atoms to diffuse towards the Mg particle core and secondly that the area of catalyst surface available for the Mg/MgH_2 reaction to occur is greatly increased by ball milling. We did not detect the presence of any metallic niobium, as found elsewhere [17].

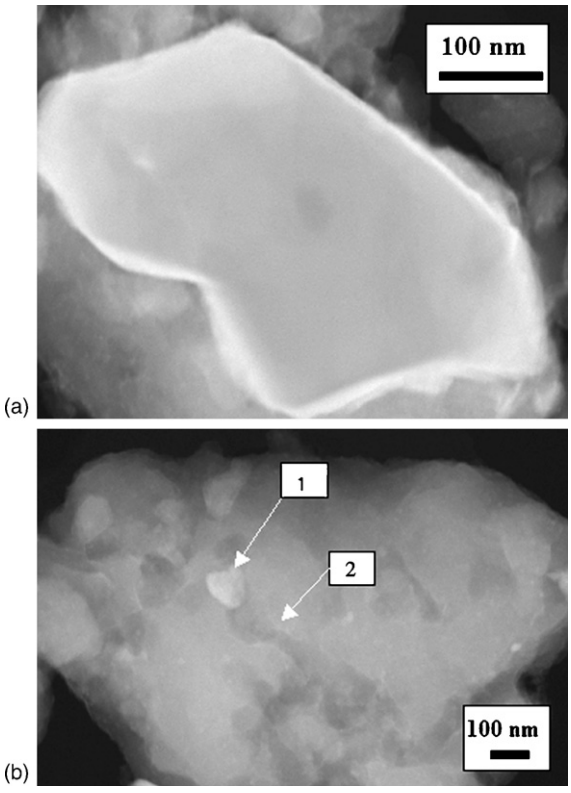

Fig. 6. (a and b) MgH_2/Nb_2O_5 thermally desorbed. HAADF micrographs of (a) bright rim around big Nb_2O_5 particles suggesting a new phase as HAADF technique does not depend on crystallographic orientations and of (b) small Nb_2O_5 particles embedded within the magnesium matrix.

3.2. *Effects of annealing*

The sample milled for 300 h was heated up to 300 °C under a hydrogen atmosphere; the hydrogen was then pumped out to initiate desorption. The HAADF image of a big catalyst particle seen in Fig. 6a reveals a bright rim all around the particle. This cannot be simple *z*-contrast because the particle itself contains the heaviest element present: Nb. Particle edges are invariably thinner with respect to the centre, so we would have expected to see a decrease in brightness at the particle edge unless there is a change in composition or structure near the surface. This layer is therefore believed to be the result of the formation of a new phase during the thermal desorption process. The corresponding HRTEM image, shown in Fig. 7, confirms the presence of a surface layer. Whereas the 0.297 nm $(\bar{3}\,1\,1)$ lattice fringes of Nb_2O_5 were detected in the particle core (A), the surface layer (B) was identified as the $MgNb_2O_{3.67}$ phase, as already found by [12], from measurement of the lattice fringe spacings and interplanar angles via a Fast Fourier Transform (FFT) of the HREM image. The presence of this phase could partially explain the catalytic effect of Nb_2O_5, as these mixed oxides are known to facilitate proton diffusion [18,19].

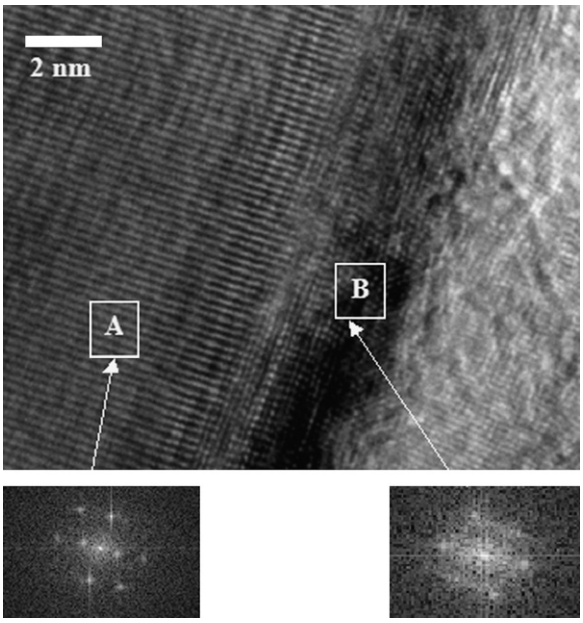

Fig. 7. MgH_2/Nb_2O_5 thermally desorbed. HRTEM micrograph of the bright rim. FFT are also shown: (A) Nb_2O_5 particle core and (B) the surface layer. FFT demonstrate the existence of a new phase.

The effect of the desorption process on the smallest Nb_2O_5 particles embedded in the Mg matrix is different; the HAADF image (Fig. 6b) shows brightest contrast around the edges of the small Nb_2O_5 particles. Again the contrast change at the particle-matrix boundary is too abrupt for a thickness effect to be the origin. HRTEM analysis carried out in the region where the bright contrast is seen demonstrates that Nb_2O_5 is still present within the magnesium matrix (dark particle): indeed, lattice fringes shown in Fig. 8a correspond exactly to (4 0 0) and (0 0 2) Nb_2O_5. However in the Mg matrix surrounding the Nb_2O_5, a new partially-reduced Nb_2O phase appears ((1 0 1) and (1 1 1)). This behaviour of niobium oxide in the magnesium matrix could be explained in these terms: the big particles (not embedded in the specimen) will come into contact with MgO amongst the surrounding Mg or MgH_2 particles so can react to form Mg-Nb-O phases, according to [18]. The finely dispersed Nb_2O_5, however, is in close contact with MgH_2 so that heating can trigger its reduction. Indeed, in situ X-ray heating experiments have shown that when an MgH_2 sample is heated to the higher temperature of 450 °C reflections appear arising from metallic Nb [17]. We have not observed any fully-reduced Nb in our samples after just a single dehydriding operation at 350 °C.

This indicates that during the desorption process Nb_2O_5 can undergo partial reduction by Mg or MgH_2 to form reduced NbO_x phases, MgO being thermodynamically more stable than Nb_2O_5. Indeed, work carried out in other laboratories has shown that when Nb_2O_5 is added to MgH_2, increased levels of MgO can be detected after H-desorption [20].

The HRTEM picture seen in Fig. 8b was recorded at the interface between an oxide particle and the Mg matrix, approximately 100 nm away from the embedded catalyst particle. It shows that Nb_2O_5 has been transformed into $MgNb_2O_{3.67}$. This product must be formed from MgO and Nb_2O_5 without reduction. Lattice fringes for Mg are also detected, corresponding to the least bright regions of the HAADF image seen in Fig. 6b.

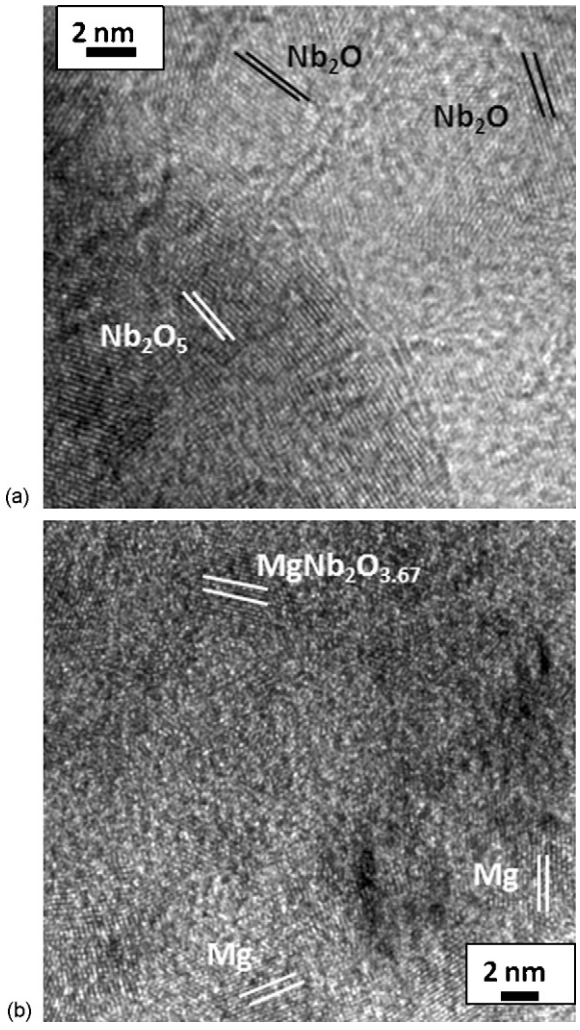

Fig. 8. MgH_2/Nb_2O_5 thermally desorbed. HRTEM micrographs of (a) the interfacial region between Nb_2O_5 and white halos and (b) the interfacial region between white halos and magnesium matrix. These micrographs refer to label 1 and 2 in Fig. 6b, respectively.

4. Conclusions

TEM-based techniques have been able to characterise catalyst structure and have clearly identified reactions between MgH_2 and Nb_2O_5. HAADF is a valuable way to locate the highly dispersed oxide phases through *z*-contrast prior to closer study using HRTEM. TEM examination showed that during the milling process Nb_2O_5 particles are broken up, eventually ending up mostly as small fragments embedded within the MgH_2. The smallest fragments probably adhere to the hydride grains and become embedded at grain boundaries when grains are welded together into larger particles. This leads to a very fine additive dispersion placed on fast diffusion paths (boundaries). It is clear that heating, even at relatively modest temperatures leads to reactions between the two compounds, with partial reduction of Nb_2O_5 to Nb_2O and production of MgO, yet unreduced

Nb_2O_5 also survives, even in the smallest particles. Interdiffusion of MgO (present in the hydride, or formed as above) and Nb_2O_5 brings about formation of the mixed oxide $MgNb_2O_{3.67}$. The exact role played by the various Nb species requires further exploration.

Acknowledgments

The work has been supported by the Research Training Network "H-Sorption in MgH_2" of the 5th Framework Programme of the EU Commission. Contract number: HPRN-CT-2002-00208. We are grateful to GKSS for provision of samples and technical advice and to Professor G.D.W. Smith for provision of laboratory facilities. M.P. wishes to thank the Electron Microscopy staff of the Department of Materials, Oxford University, for technical support.

References

[1] B. Bogdanovic, B. Splichthoft, Angew. Chem. 29 (3) (1990) 223.
[2] J. Huot, G. Liang, S. Bobet, A. Van Neste, R. Schultz, J. Alloys Compd. 295 (1999) 495.
[3] J. Huot, G. Liang, S. Bobet, A. Van Neste, R. Schultz, J. Alloys Compd. 292 (1–2) (1999) 247.
[4] W. Oelerich, T. Klassen, R. Bormann, J. Alloys Compd. 315 (2001) 237.
[5] A.R. Yavari, J.F.R. de Castro, G. Vaughan, G. Heunen, J. Alloys Compd. 353 (1–2) (2003) 246.
[6] C. Suryanarayana, Prog. Mater. Sci. 46 (2001) 1.
[7] D. Fatay, A. Revesz, T. Spassov, J. Alloys Compd. 399 (2005) 237.
[8] G. Barkhordarian, T. Klassen, R. Bormann, J. Alloys Compd. 364 (2004) 242.
[9] D.B. Williams, C.B. Carter, Transmission Electron Microscopy: A Textbook for Materials Science, Plenum Press, New York, 1996.
[10] B. Bokhonov, E. Ivanov, V. Boldyrev, Mater. Lett. 5 (5–6) (1987) 218.
[11] C.M. Andrei, J. Walmsley, D. Blanchard, H.W. Brinks, R. Holmestad, B.C. Hauback, J. Alloys Compd. 395 (1–2) (2005) 307.
[12] O. Friedrichs, J.C. Sánchez-López, C. López-Cartes, M. Dornheim, T. Klassen, R. Bormann, A. Fernández, Appl. Surf. Sci. 252 (6) (2006) 2334.
[13] P.J. Herley, W. Jones, Zeit Phys. Chem. 147 (1986) 785.
[14] S.J. Pennycook, D.E. Jesson, Phys. Rev. Lett. 64 (1990) 938.
[15] J.R. Ares Fernandez, F.-K. Aguey-Zinzou, unpublished results.
[16] J.R. Ares, K.-F. Aguey-Zinzou, T. Klassen, R. Bormann, J. Alloys Compd. 434-435 (2007) 729.
[17] O. Friedrichs, K.-F. Aguey-Zinzou, J.R. Ares Fernandez, J.C. Sanchez Lopez, A.J. Erbez, T. Klassen, R. Bormann, A.F. Camacho, Acta Mater. 54 (2006) 105.
[18] F. Abbattista, P. Rolando, G. Borroni Grassi, Ann. Chim. 60 (1970) 426.
[19] J.B. Goodenough, Rep. Prog. Phys. 67 (2004) 1915.
[20] MgH_2 Research Training Network Web Page: http://www.inpg.fr/RTN-MgH2/ Contents Section.